crystals

MDPI

Article

Gemology, Mineralogy, and Coloration Mechanism of Pinkish-Purple Cobaltoan Dolomite from the Democratic Republic of Congo

Ying Yan and Xiao-Yan Yu *

School of Gemology, China University of Geosciences Beijing, 29 Xueyuan Road, Beijing 100083, China; 2009210031@email.cugb.edu.cn
* Correspondence: yuxy@cugb.edu.cn

Abstract: A pinkish-purple cobaltoan dolomite from the Democratic Republic of Congo (DRC) has appeared on the Chinese gemstone market recently. In this study, Raman analysis spectroscopy, Fourier transform infrared (FTIR) spectroscopy, electron probe micro-analysis (EPMA), scanning electron microscopy (SEM), energy-dispersive X-ray fluorescence (EDXRF), and fiber optic spectrometry were used to explore the gemology, mineralogy, and coloration mechanism of cobaltoan dolomite. Results indicate that cobaltoan dolomite is a mineral aggregate with a granular texture. The degree of fineness and luster differs due to mineral (quartz) impurities in the texture. The cobaltoan dolomites are typically associated with carbonates, such as azurite, malachite, spherocobaltite, and the rare species kolwezite, which were documented in this study. The natural presence of magnesite-spherocobaltite solid solution with distinct chemical zoning occurs as crystals in the country rock. The pinkish-purple dolomites are mainly colored by CoO, whose concentrations ranged from 0.966 to 6.111 wt.%. Based on UV-Vis spectroscopy, cobaltoan dolomite showed broad characteristic absorption bands at 531.5 nm, which varied as the concentrations of CoO increased. The origin of the color is related to the electronic transition of Co^{2+} and charge transfer between the ions.

Keywords: cobaltoan dolomite; Co ions; gemological properties; mineral composition;coloration mechanism

Citation: Yan, Y.; Yu, X.-Y. Gemology, Mineralogy, and Coloration Mechanism of Pinkish-Purple Cobaltoan Dolomite from the Democratic Republic of Congo. *Crystals* **2022**, *12*, 639. https://doi.org/10.3390/cryst12050639

Academic Editors: Taijin Lu, Fei Liu, Tingting Gu and Sergey V. Krivovichev

Received: 18 February 2022
Accepted: 24 April 2022
Published: 29 April 2022

1. Introduction

Cobaltoan dolomite is a pink to purple variety of dolomite. Similar to cobaltocalcilte, the gem is popular for its striking purplish pink color caused by the presence of cobalt in the crystal structure [1]. Dolomite is widely used in daily life, including in building materials, ceramics, and inorganic nonmetals. The mineral has given rise to several professional fields of study [2]. However, cobaltoan dolomite, a Co-rich member of the dolomitic group of minerals in carbonates, is currently the only dolomite used as a gem material in the world. Minerals of the dolomite group, with the general formula $AB(CO_3)$, comprise common phases, such as ankerite and kutnahorite [3]. The ideal chemical formula is $CaMg[CO_3]_2$ [4]. Dolomites hosting Me^{2+}, such as those with Zn and Co substituting for the octahedral Mg^{2+}, are commonly found in the supergene oxidation zones of sulfide deposits [5]. Co ions occurs in dolomite in octahedral coordination [6].

At present, cobaltoan dolomite mainly occurs in the Democratic Republic of Congo, and is characterized by copper-cobalt polymetallic deposits occurring in Neoproterozoic sedimentary rocks [7]. Cobaltoan dolomite is found in several localities in the Central African Copperbelt [8–11] stretching across the border between Zambia and the Democratic Republic of Congo. It is one of the largest sediment-hosted stratiform Cu-Co provinces globally [12]. Cobaltoan dolomites are typically associated with carbonates, such as the common species malachite and azurite [13], and the rare species kolwezite and carrollite [14,15]. As a new gem material, cobaltoan dolomite has appeared on the Chinese

jewelry market in recent years. The gem displays an attractive pale pink to purplish color, which is very alluring to people. However, it is very similar to some usual gems, such as sugilite, rhodonite, and rhodochrosite, resulting in confusion on the jewelry market and causing difficulties in terms of identification [16].

Several previous studies on cobaltoan dolomite focused only on geochemistry, metallurgy, and crystal structure analysis, whereas studies on gemology, spectroscopy, and coloration mechanism are still relatively scarce at present. For example, through SEM/EDAX studies, Douglass identified a pink mineral of cobalt-rich dolomite from Kamoto mine (DRC), previously described as cobalt-rich calcite [17]. A crystal structure study was documented by Perchiazzi [18] for cobaltoan dolomite from Kolwezi (DRC). Minceva-Stefanova [19] reported an EPMA study of cobaltoan dolomite crystals from unknown regions, showing the presence of alternating chemical zonings with an overall increase in Co content from the core to the rim. A more detailed data set was reported by Barton for cobaltoan dolomite from the Democratic Republic of Congo, with CoO content ranging up to 11.41 wt.%, and provides the chemical composition of magnesite-spherocobaltite solid solution [20]. A full crystal-chemical study of cobaltoan dolomite was first reported by Perchiazzi et al. [21], which provides a model for analyzing the crystal structure of cobaltoan dolomite.

Cobaltoan dolomite has been on the jewelry market for a short time, and there is still not a systematic study on it as an independent gemstone variety. The gemological properties of the gem are not clear, which not only makes it difficult to identify, but also restricts the further development and utilization of cobaltoan dolomite resources. Therefore, in this research, representative samples of cobaltoan dolomite from the Democratic Republic of Congo were collected. Samples were analyzed to provide data for the scientific identification, evaluation, and further development of cobaltoan dolomite. Firstly, standard gemological analyses were used to study the samples' appearance and gemological properties. Microstructure characteristics and processing properties of the samples were then analyzed using a polarizing microscope and SEM. Later, the mineral composition was determined using Raman spectroscopy, FTIR, and EPMA. Finally, by combining XRF and UV-Vis, the coloration mechanism of cobaltoan dolomite was analyzed.

2. Materials and Methods

2.1. Materials

Nine coboaltoan dolomite samples covering all color varieties were selected, including pink, pink with disseminated blue, reddish-purple, and purple (Figure 1). The samples comprised four polished samples (D1–D4) and five rough stones (R1–R5).

Figure 1. Selected nine samples of cobaltoan dolomites with different colors.

2.2. Methods

2.2.1. Standard Gemological Analyses

The refractive index (RI) and specific gravity (SG) of the samples were measured by the distant vision and hydrostatic weighing methods, respectively. The ultraviolet fluorescence was measured by the ultraviolet lamp analyzer. The samples were observed under a GI-MP 22 gemological microscope using reflected light.

2.2.2. Microstructure and Spectroscopy Characteristics of Cobaltoan Dolomite

Parts of the samples with characteristic colors were selected from samples (R1, R2) to prepare petrographic thin sections. The thin sections were observed and photographed using a BX51 polarized light microscope (PLM).

Raman microprobe spectra were tested with an Horiba LabRAM HR-Evolution laser Raman spectrometer. The analytical conditions used for measurement included a range of 100–2000 cm^{-1}, an accumulation time of 3 s, a laser wavelength of 532 nm, and a grating of 600 (500 nm).

Scanning electron microscopy (SEM) was performed by Zeiss SUPRATM 55 thermal field emission high-resolution scanning electron microscope (SEM) with a resolution of 0.8 mm, an accelerating voltage of 0.1~30 kV, and a detection element range of Be (4)-U (92).

The Bruker Tensor 27 Fourier transform infrared spectrometer from Germany was used for infrared spectrum test by direct reflection method. Analytical conditions included a scan range of 400–2000 cm^{-1}, a resolution of 4 cm^{-1}, and a run time of 30 s per scan.

2.2.3. Chemical Composition Characteristic of Cobaltoan Dolomite

The chemical analyses of samples were conducted using a JXA-8230 electron microprobe (EPMA) at the Key Laboratory of Metallogeny and Mineral Assessment, Institute of Mineral Resources, Chinese Academy of Geological Science (CAGS). The operating conditions were as follows: an accelerating voltage of 15 kV, a beam current of 20 nA, and a beam diameter of 1–5 μm. Peak and background counting times were 10 s and 5 s, respectively.

2.2.4. Coloration Mechanism of Cobaltoan Dolomite

Semiquantitative element testing was performed using the EDX-7000 X-ray fluorescence (EDXRF) manufactured by Shimadzu Corporation of Japan. The main operating conditions were as follows: electron beam energy, 2.2 KeV; X-ray energy range, 3.5~35 keV; detector, Si (Li); collimator, 1 mm; atmosphere, vacuum.

UV-Vis Spectrum: The absorption spectrum in the UV-Vis range was tested with a Gem-3000 fiber optic spectrometer (Biaoqi Optoelectronics Technology Development Co., LTD., Guangzhou, China). The test conditions are as follows: wavelength range, 300–1000 nm; integral time, 200 s; average scan turns, 10; boxcar width, 2.

3. Results and Discussion

3.1. Sample Appearance and Gemological Properties

The pink sample (D1) of delicate texture and smooth surfaces consisted mainly of pink basal minerals (Figure 2a). The sample's color is uneven. A minority of black and blue paragenetic minerals can be seen in D1, presenting a bright glassy luster (Figure 2b). The sample (D2) consisted mainly of pink basal minerals with maroon plaques (Figure 2c). There are a number of gray grain minerals near the reddish-purple sample (D3), with a coarse texture (Figure 2d). In addition, some distinct dark purple veining striations are distributed on the surface of the sample (D3). The luster of D2 and D3 was dimmer than that of the samples. Raw gemstone samples R1 and R2 were cut for microsection observation. Sample R1 consisted mainly of the pink matrix with green country rock, whereas sample (R2) consisted mainly of pink basal minerals. The light pink sample (R3) consisted mainly of pink and gray basal minerals, black spots, and small green mineral grains (Figure 2e).

The pinkish-purple sample (R4) consisted mainly of pink and black minerals (Figure 2f) whose grain size was larger than those of the rest of the samples. There are clear reflecting surfaces in the shape of "fly wings" on the rock sample R4 as viewed under reflected light (Figure 2f), indicating that the cleavage of the basal minerals is well developed [22].

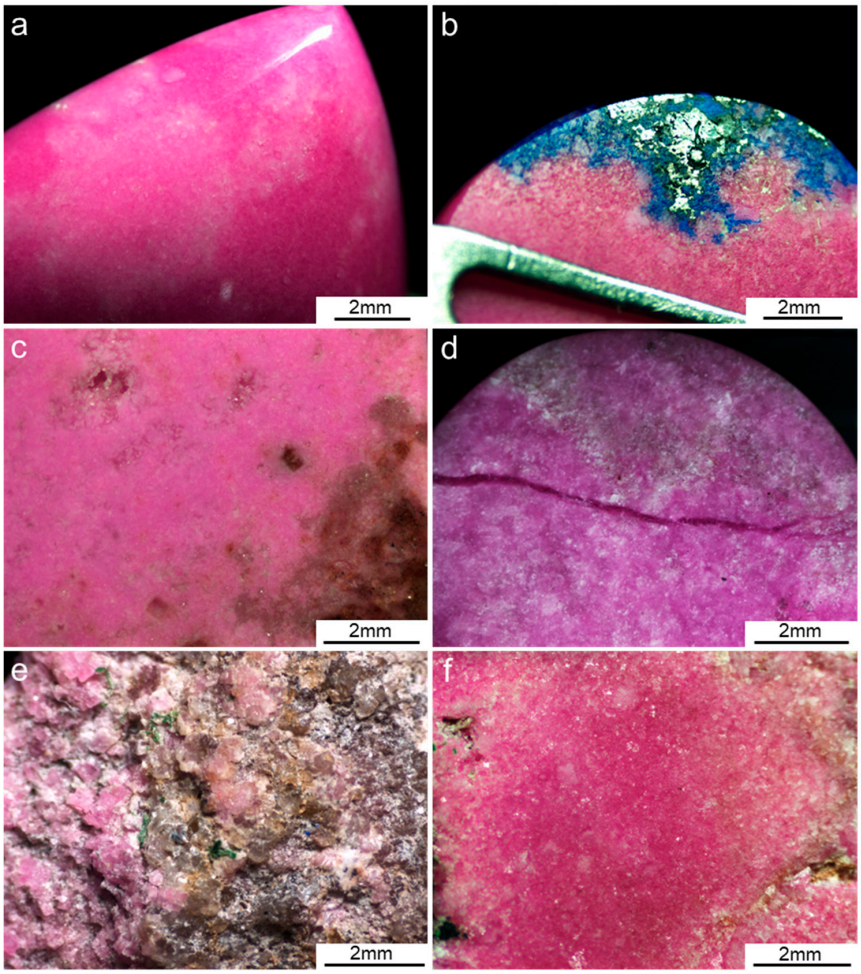

Figure 2. Sample appearance: (**a**). The smooth surfaces and uneven color of D1; (**b**). The black and blue paragenetic minerals display a bright glassy luster; (**c**). The maroon plaque minerals on D2; (**d**). The gray grains and dark purple veining on D3; (**e**). The pink and gray basal minerals on R3; (**f**). Image of the "fly wings" reflecting surfaces on the sample R4.

The gemological properties of the samples are presented in Table 1. Dolomite is a tripartite crystalline mineral. Cobaltoan dolomites are opaque, mostly of glass luster, and rough in texture. All samples are non-fluorescent under the UV lamp. The paragenetic minerals make the surfaces of samples display a different luster, further influencing the refractive index. The refractive index of the cobaltoan dolomite ranges from 1.51 to 1.57. The specific gravity (SG) of the samples ranges from 2.81 to 2.86. Compared with the 2.85 value of the theoretical relative density of dolomite [4], sample R3 is much lower, which is affected by the large number of gray paragenetic minerals in the basal.

3.2. Microstructure and Spectroscopy Characteristics

3.2.1. Microstructure Characteristics

Observation of the samples under a gemological microscope revealed that the color of the pinkish-purple matrix was not uniform, with different shades visible on the surface of blue, green, black, white, and other associated minerals. The cobaltoan dolomites studied in this paper are all naturally occurring mineral aggregates. The content of dolomite in each

sample is different, and samples contain different amounts of impurity minerals, resulting in different values of specific gravity and refractive index across samples [23].

Table 1. Conventional gemological properties of cobaltoan dolomite samples.

Sample Number	Color	Luster	Transparency	Refractive Index	Fluorescence	Specific Gravity
D1	pink; blue	vitreous luster	opaque	1.55	None	2.85
D2	pink	subvitreous luster	opaque	1.51	None	2.81
D3	reddish-purple	oil-subvitreous luster	opaque	1.52	None	2.84
D4	deep purple	vitreous luster	opaque	1.57	None	2.86
R1	pink; green	vitreous luster	opaque	-	None	2.85
R2	pink	vitreous luster	opaque	-	None	2.83
R3	light pink	vitreous luster	opaque	-	None	2.78
R4	pink	vitreous luster	opaque	-	None	2.83
R5	pink	vitreous luster	opaque	-	None	2.82

Figure 3 show the mineral microstructure and paragenetic relationships of the samples. The blue part of sample D1 shows a prominent dissemination structure (Figure 3a), and the texture is relatively coarser near the disseminated mineral. Combined with the microscopic laser Raman spectrum test, its characteristic peaks are located at 392, 1093, 1436, and 1571 cm^{-1} (Figure 4a), which is consistent with the Raman characteristic peaks of azurite in the "RRUFF" mineralogy database. An irregular distribution of green minerals with silky luster can be seen on the surface of rough stones (Figure 3b). The Raman characteristic peaks of green minerals are located at 151, 218, 430, 1066, 1094, and 1363 cm^{-1} (Figure 4b). The green minerals were then determined to be malachite. Due to the unpolished surface of the tested rock samples, there are some minor deviations and miscellaneous peaks in the Raman displacement range.

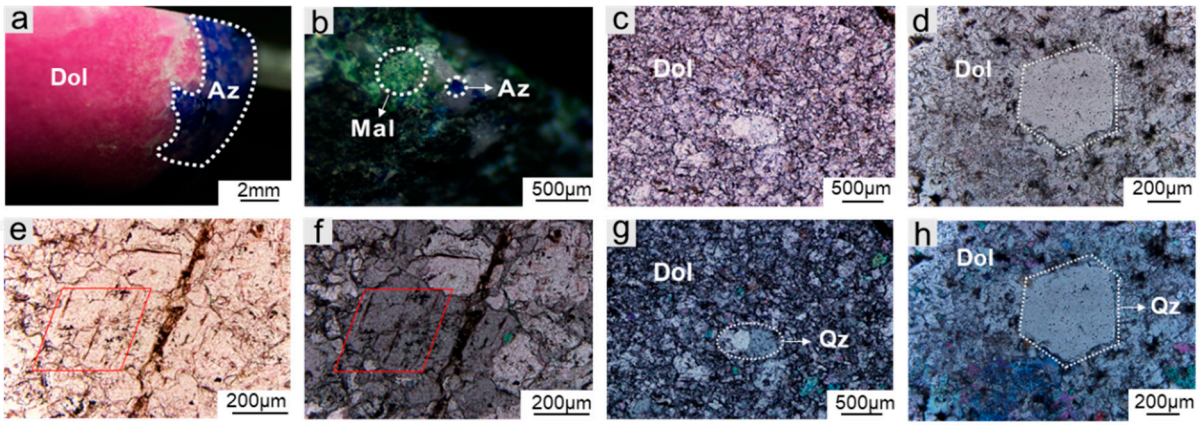

Figure 3. Mineral microstructure and paragenetic relationships of the sample: (**a**). The dissemination structure of azurite and dolomite in sample D1; (**b**). Associated minerals (Az, Mal) in country rock of sample R5; (**c**). Microstructure of R2 sample under plane-polarized transmitted light; (**d**). Idiomorphic quartz grains under plane-polarized transmitted light; (**e**). Rhomboid cleavage of dolomite under plane-polarized transmitted light; (**f**). Rhomboid cleavage of dolomite under cross-polarized transmitted light; (**g**). Microstructure of R2 sample under cross-polarized transmitted light; (**h**). Idiomorphic quartz grains under cross-polarized transmitted light. Mineral abbreviations: Dol = Dolomite; Az = Azurite; Mal = Malachite; Qz = Quartz.

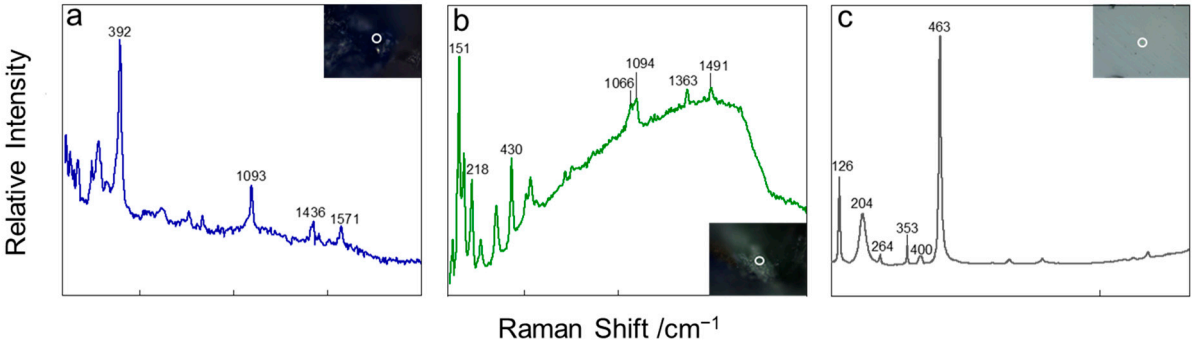

Figure 4. The Raman microprobe spectra for different minerals in the rock samples. (**a**). Azurite; (**b**). Malachite; (**c**). Quartz.

Figure 3c,d show the mineral microstructural characteristics and paragenetic relationships of sample R2. Here, the size of dolomite crystals ranges from tens of micrometers to a few millimeters, and there is no clear orientation between grains. Under plane-polarized light, cobaltoan dolomite presents as light pink, and an irregular distribution of euhedral–allotriomorphic gray granular minerals can be observed in the matrix. Dolomites usually have complete cleavage in the {1010} direction and two sets of oblique rhomboid cleavage lines exist [24]. However, dolomite grains in the sample R2 are generally small in diameter due to incomplete development. Two sets of oblique rhomboid cleavage lines can be found only when the local particle size is up to 150–300 μm (Figure 3e,f). Under crossed polarized light, the euhedral–allotriomorphic gray granular minerals present with positive low protrusion and high white interference color (Figure 3g,h). Raman spectroscopy was used to determine that the paragenetic mineral was quartz. The Raman spectra are consistent with peaks of quartz at 126, 204, 264, 353, 400, and 463 cm^{-1} (Figure 4c). The assignment of specific Raman shifts of different minerals are listed in Table 2. Thin-section investigation revealed that cobaltoan dolomite is granular in shape with a grain size of about 0.1–0.3 mm. Dolomite is present in samples in the form of the matrix, and it is the major mineral of the samples. The pink portion mainly depicts a close association between dolomite and the different forms of quartz.

Table 2. The assignments of the different minerals (after Raman microprobe measurement).

Minerals	Raman Shift, cm^{-1}	Assignment	Reference
Azurite	1093	V_1 (C–O)	[25]
	1436	V_3 (C–O)	
	1571	V_{as} (CO_3^{2-})	
	392	V_s (Cu–O)	
Malachite	1066, 1094	V_s (C–O)	[26]
	1491	V_3 (CO_3^{2-})	
	430	V_s (Cu–OH)	
	218	Bending vibration of O–Cu–OH	
	151	Bending vibration of O–Cu–O/OH	
Quartz	126, 204	$[SiO_4]_R/[SiO_4]_T$	[27,28]
	463	V_s (T–O–T)	
	264, 353, 400	V_s (Si–O)	

Moreover, the presence of impurity mineral quartz leads to a difference in hardness, which affects the smoothness after polishing [29]. Combined with scanning electron microscopy, the gray surface area of the quartz-containing sample D3 was observed to be rough (Figure 5a), displaying an oil–subvitreous luster (RI is 1.52). However, the surface of sample D1, which does not contain quartz impurities, was smooth (Figure 5b) and exhibited a vitreous luster (RI is 1.55). Therefore, quartz is the primary cause of the micro pits on

the sample surfaces. The degree of crystallization of quartz particles affects the texture, structure, and luster of polished cobaltoan dolomites samples.

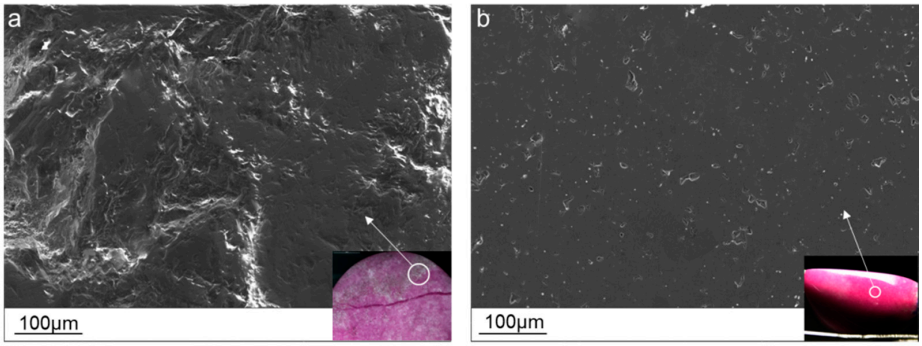

Figure 5. SEM images of the polished surface of cobaltoan dolomite: (**a**). The part with high quartz content is coarser; (**b**). The part with low quartz content is smoother.

3.2.2. FTIR Spectra

Different color parts of cobaltoan dolomites were selected for Infrared spectrum testing to determine the textural relationships to other paragenetic associated minerals. Figure 6 shows typical FTIR spectra in the range of 2000–400 cm^{-1}.

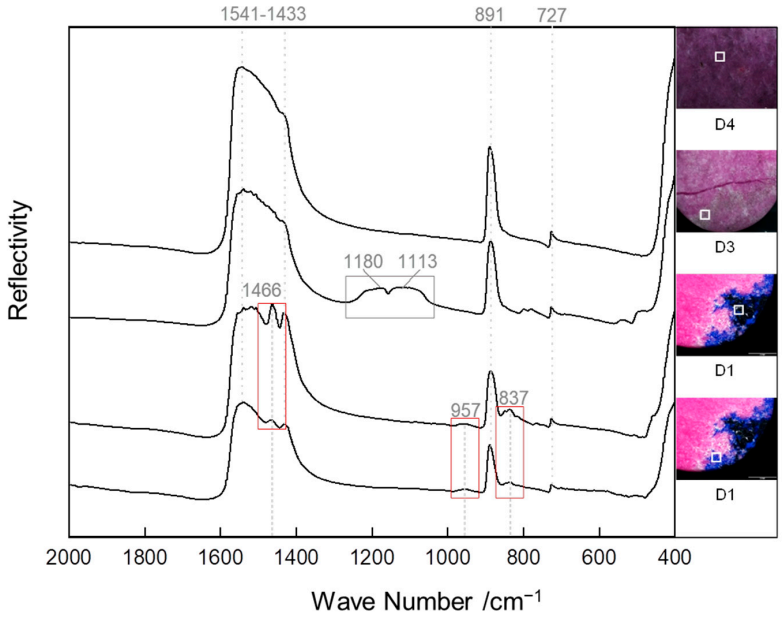

Figure 6. Infrared spectra of samples (D1, D3, D4) in different colors. The spectra are displaced vertically for clarity.

According to Gunasekaran [30], the infrared spectrum of dolomite displays sharp absorption peaks that appear at approximately 728, 879, and 1433 cm^{-1}. The infrared spectra of the natural dolomite samples are quite similar. With a broad absorption band of 1541–1433 cm^{-1} and sharp peaks at 727 and 891 cm^{-1} in the range of 900–600 cm^{-1} [31]. The peak at 891 cm^{-1} of $\nu(CO_3^{2-})$ is sharp and strong [32], and the absorption of ν(O–C–O) near 727 cm^{-1} is sharp but weak [33]. The absorption of ν(C–O) in the 1541–1433 cm^{-1} range is wide and strong [34]. The three characteristic absorptions of the samples correspond to the asymmetric stretching of ν(C–O).

The infrared spectra of the gray (D3) and blue (D1) parts are slightly different from the purple part (D4). The gray part has clear absorption double peaks at 1180 and 1113 cm^{-1}, which is related to the antisymmetric stretching vibration of Si–O–Si in quartz [35]. There

are 1466 cm^{-1}, 957 cm^{-1}, and 837 cm^{-1} characteristic spectrum peaks of azurite in the blue and black parts. The 837 and 957 cm^{-1} are attributed to the out-of-plane and in-plane bending vibration modes of carbonate ion (V_2), and the absorption at 1466 cm^{-1} is the asymmetric bending vibration of C–O (V_3) [26]. Because the disseminated mineral in sample D1 is often in the form of crystals with very small particle sizes, the dissemination area is large but the total content is low, and it is difficult to identify them qualitatively by just the results of infrared spectroscopy. Combined with the previous Raman spectroscopy analysis, the disseminated minerals were then determined to be azurite. The assignments of dolomite, quartz, and azurite are listed in Table 3.

Table 3. The assignments of the different minerals (after FTIR Spectra measurement).

Minerals	Wave Number, cm^{-1}	Assignment	Reference
Dolomite	1541, 1433	V (C–O)	[32–34]
	891	V (CO_3^{2-})	
	727	V (O–C–O)	
Quartz	1180, 1113	V_s (Si–O–Si)	[35]
Azurite	1466	Asymmetric bending vibration of C–O	[26]
	957, 837	V_2 (CO_3^{2-})	

3.3. Electron Microprobe Analyses

Cobaltoan dolomite from the Democratic Republic of Congo occurs as a pink to purple aggregate, and there are abundant paragenetic minerals, so the chemical composition is complex. Figure 7a shows the backscattered electron image of the transition environment between the dolomite matrix and the green country rock. Each image is labeled with a corresponding tag. Table 4 shows the representative composition of the dolomite matrix in this study. The main chemical composition of dolomite is $CaMg[CO_3]_2$. The dolomite in the samples consists (wt.%) of MnO (0.106~0.217), CoO (0.966~6.111), MgO (16.346~20.057), and CaO (28.529~29.934). The star-dotted basal minerals consist (wt.%) of CoO (37.348~37.449), MgO (15.229~15.297), and CaO (1.640~2.224), in which the MgO concentration is relatively higher than its content in an ideal spherocobaltite ($CoCO_3$). So, the matrix of the sample R1 is mainly composed of dolomite and star-dotted Mg-rich spherocobaltite (Figure 7b). Barton et al. (2014) showed evidence of textural similarity to the Mg-rich spherocobaltites formed by the dedolomitization of dolomite, and cobaltoan dolomite and Mg-rich spherocobaltites are surely the products of primary precipitation [20]. Dedolomitization is a common geological phenomenon in the supergene environment and is also another mechanism for creating $(Mg,Co)CO_3$. Therefore, the presence of magnesium-rich spherocobaltites makes it possible to indicate cobaltoan dolomite formation in the supergenetic environment.

Table 4. Chemical composition (wt.%) of the cobaltoan dolomite sample matrix investigated, obtained through EPMA analyses.

Sample; Mineral [1]	R2-a-1; Dol	R2-a-2; Dol	R2-a-3; Dol	R2-b-1; Sph	R2-b-2; Sph
NaO	0.035	0.029	0.037	0.086	0.090
MgO	17.769	20.057	16.346	15.297	15.229
CaO	29.209	29.934	28.529	1.64	2.224
TiO_2	0.047	0.071	0.000	0.061	0.051
MnO	0.119	0.152	0.106	0.217	0.148
FeO	1.574	0.426	0.062	0.072	0.147
CoO	2.532	0.966	6.111	37.449	37.348
total	51.285	51.635	51.191	54.822	55.237

[1] Mineral abbreviations: Dol = Dolomite; Sph = Spherocobaltite.

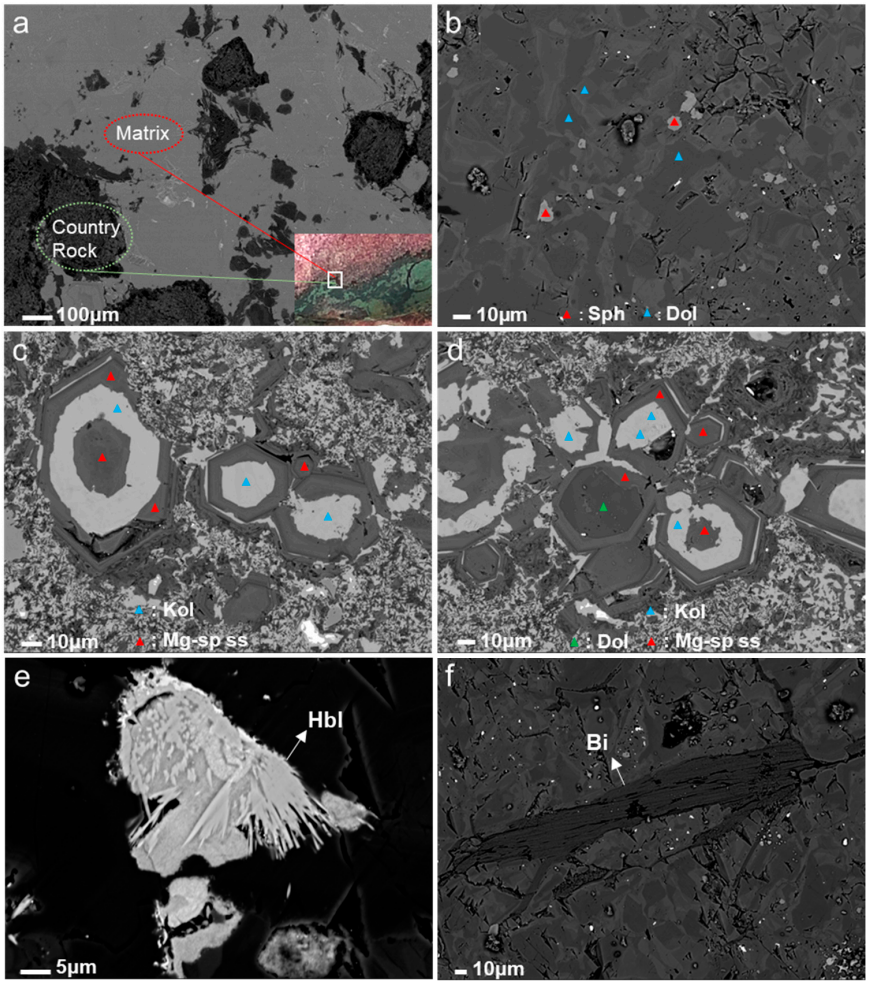

Figure 7. Backscatter images of cobaltoan dolomite: (**a**). The transition environment between dolomite matrix and green country rock of sample R1; (**b**). Dolomite and spherocobaltite are distributed on the matrix; (**c**). Image of the chemical zoning in country rock; (**d**). Image of the chemical zoning in country rock; (**e**). Image of the altered hornblende; (**f**). Image of the biotite with a group of perfect cleavage. Mineral abbreviations: Dol = Dolomite; Sph = Spherocobaltite; Mg-sp ss = Magnesite-spherocobaltite solid solution; Kol = kolwezite; Hbl = Hornblende; Bi = Biotite.

Clearer backscatter electron probe images of chemical zoning in the sample's country rock are also reported. There are strong compositional zonings that were tested to be a reaction rim texture formed by dolomite, kolwezite, and other special crystal interpenetration metasomatism residues (Figure 7c,d). The zoning has a complete hexagonal structure and is concentric about the c-axis of several crystals. The representative compositions of the minerals are shown in Table 5. Besides the documented dolomite compositions, this study shows the occurrence of special crystal specimens in a solid solution between magnesite and sphaerocobaltite, presenting distinct chemical zoning within single crystals, mainly containing MgO (25.600~30.296 wt.%) and CoO (21.028~26.447 wt.%). The main chemical composition of kolwezite mineral is $(Cu,Co)_2(CO_3)(OH)_2$, and consists (wt.%) mainly of CuO (56.966~63.032), CoO (2.974~6.204).

The transition metal carbonates have extensive solid solutions. Goldsmith and Northrop indicated a theoretical complete solid solution between magnesite and sphaerocobaltite and were the first to report the occurrence of $(Mg,Co)CO_3$ [36]. The presence of solid solution confirms that the sample was formed in a low-temperature epiphytic environment [20]. Furthermore, no data exist on the composition of kolwezite in the Copperbelt to date, and the only specimens available at TFM were the kolwezite-magnesian spherocobaltite inclusion, in which the kolwezite proved too small to analyze. In this

study, kolwezite appeared in the chemical zoning in country rock for the first time, and the crystal size was up to 30 microns. Under such a condition the new data on the chemical composition of kolwezite were documented (Table 5).

Table 5. Chemical composition (wt.%) of the zoning in the country rock investigated, obtained through EPMA analyses.

Sample; Mineral [1]	R1-a-1; Mg-sp ss	R1-a-2; Mg-sp ss	R1-a-3; Mg-sp ss	R1-a-4; Mg-sp ss	R1-a-5; Kol	R1-a-6; Kol	R1-a-7; Kol	R1-b-1; Dol
NaO	0.188	0.269	0.187	0.268	0.180	0.260	0.142	0.115
MgO	28.600	26.038	27.080	25.600	0.626	0.783	2.511	19.925
SiO_2	0.175	0.054	0.216	0.123	0.035	0.141	0.025	0.026
CaO	0.921	0.185	1.006	0.221	0.002	0.028	0.002	30.524
TiO_2	0.011	0.000	0.064	0.000	0.030	0.000	0.000	0.000
MnO	0.035	0.050	0.122	0.077	0.000	0.003	0.017	0.027
FeO	0.000	0.028	0.028	0.058	0.129	0.113	0.068	0.020
CoO	21.028	25.939	24.071	26.447	2.974	4.608	4.568	1.496
NiO	0.000	0.595	0.096	0.915	0.000	0.000	0.000	0.022
CuO	1.043	1.059	0.872	1.014	63.032	60.632	59.718	1.015
total	52.001	54.217	53.742	54.723	67.008	66.568	67.051	53.170
NaO	0.127	0.310	0.109	0.333	0.125	0.094	0.288	0.402
MgO	27.600	27.093	30.296	26.605	25.619	0.623	1.146	1.111
SiO_2	0.022	0.140	0.029	0.206	0.027	0.069	0.066	0.049
CaO	0.695	1.121	0.169	0.949	0.131	0.014	0.049	0.043
TiO_2	0.053	0.000	0.000	0.063	0.000	0.040	0.040	0.040
MnO	0.154	0.059	0.107	0.165	0.081	0.037	0.005	0.023
FeO	0.000	0.000	0.000	0.003	0.027	0.000	0.000	0.061
CoO	24.030	23.875	21.594	24.549	25.339	5.417	6.204	6.136
NiO	0.410	0.278	0.833	0.133	0.613	0.000	0.000	0.000
CuO	0.655	0.715	0.868	0.820	2.433	60.265	56.966	59.074
total	53.746	53.591	54.005	53.826	54.395	66.559	64.764	66.939

[1] Mineral abbreviations: Dol = Dolomite; Mg-sp ss = Magnesite-spherocobaltite solid solution; Kol = Kolwezite.

In addition, paragenetic silicate minerals, such as altered hornblende (Figure 6e) and a group of perfect cleavage biotite (Figure 6f), were also found in the green country rock. These typical metamorphosed minerals can be used as prospecting indicators of Cu-Co deposits occurring in the Democratic Republic of Congo [11]. This study showed that cobaltoan dolomite often exists in association with azurite, malachite, and kolwezite. Azurite and malachite occur in the supergene zones of Cu-Co sulfide ore deposits, originating from the alteration of primary sulfides, such as chalcocite, carrollite, and Cu $(Co,Ni)_2As_4$ [18]. The well-formed cobaltoan dolomite crystals are most common in the supergene zones of Cu-Co sulfide ore deposits in the Democratic Republic of Congo [37]. Therefore, the typical mineralization characteristic of cobaltoan dolomite is particularly significant in the vicinity of the speckled copper-cobalt ore. Members of the magnesite-spherocobaltite solid solution occur as crystals filling void spaces in rocks and as microscopic inclusions with kolwezite in supergene chalcocite (Cu_2S) replacing primary carrollite ($CuCo_2S_4$) [20]. The existence of solid solution confirmed the nature of mineralization of cobalt-rich carbonate minerals that occur in sulfide deposits. The mineral composition characteristics of the cobaltoan dolomite are consistent with the geological setting in the Democratic Republic of Congo and provide new data on the mineral characteristics of the samples' formation environment.

3.4. Analysis of Coloration Mechanism

In the ideal ordered dolomite lattice structure, magnesium and calcium occupy different layers [38] (Figure 8a). Mg in dolomite can be substituted with Fe, Mn, Co, and Zn isomorphism, which affects the crystal structure of dolomite, thus causing the difference in the physical properties of dolomite. The color of dolomite with different components is varied. Ferric dolomite is yellow-brown and manganese-bearing dolomite is red [4].

Moreover, the change in the color of the cobalt metal complex may be due to the complex coordination number. A pink or red cobalt compound has a coordination number of 6, while a blue one has a coordination number of 4 or 3 [39]. As the name implies, cobaltoan dolomite refers to the presence of Co element in dolomite in the form of a regular octahedral coordination ion configuration with a coordination number of 6 (Figure 8b).

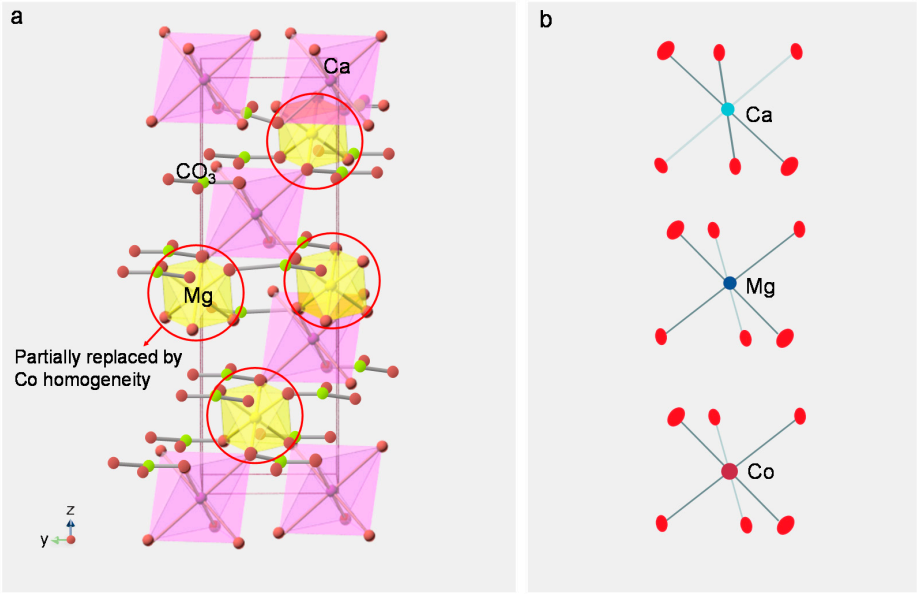

Figure 8. (**a**). The crystal structure of cobaltoan dolomite; (**b**). Coordination polyhedra model in cobaltoan dolomite (referring from Perchiazzi [18]).

Energy-dispersive X-ray fluorescence (EDXRF) spectrometry is a quick and non-destructive means of detecting the presence of most elements in cobaltoan dolomite. Four polished samples were semiquantitatively analyzed using EDXRF (Table 6). Besides the main constituent calcium and magnesium, regular pinkish-purple cobaltoan dolomite samples tended to have high concentrations of CoO (1.07–8.70 wt.%). The contents of MgO (31.93 to 39.15 wt.%) were negatively related to CoO, while the CoO/MgO ratio regularly ranged from 0.03 to 0.27. The blue part of sample D1 showed high concentrations of CuO (avg. 55.02 wt.%), related to the large area of epigenetic azurite leaching.

Comparing the hand specimen observation, it was found that the color of samples was changed with the increase in CoO/MgO ratio. This study further found that the CoO/MgO ratio reflects the degree of isomorphic substitution of magnesium by cobalt in dolomite crystals. Comparing the color of the hand specimen, purple deepened with the increase in CoO/MgO ratio, implying that Co ions concentration has an impact on coloration. Co ions influence the color of the sample similar to the combination of chromatin elements in cobaltocalcite studied by preceding researchers [1]. However, they still found some Mn (reaching up to 8719 ppmw) in cobaltocalcite and asserted that, given appropriate concentrations, manganese can cause the pink to purple color. The results of EPMA (Table 4) and EDXRF (Table 6) from the cobaltoan dolomite showed very low concentrations of MnO (avg. 0.20 wt.%) and high contents of CoO (avg. 4.93 wt.%). The content trend of MgO with the color of samples was not clear. Thus, Co is the main coloring element in dolomite, and Mn has relatively little influence.

To further analyze and discuss the influence of Co ions on the color of opaque cobaltoan dolomite, UV-Vis spectra tests were carried out on the corresponding representative composition test points. The UV-Vis spectrum of the opaque pinkish-purple samples (Figure 9) showed a dominant region absorption band at 531.5 nm. The sample's purple color is gradually saturated from the bottom to the top, and the spectra show a low-to-high absorbance trend at 531.5 nm. The chemical analysis (EDXRF) was normalized to a ratio of

CoO/MgO (Figure 9, inset). Results show that the pinkish-purple sample's higher concentration is consistent with a higher CoO/MgO ratio level, producing a more saturated color. The concentration of CoO is consistent with the intensity of the 531.5 nm absorption bands in the visible region of samples (D1–D4). Accordingly, the color of cobaltoan dolomite is positively correlated with the content of CoO and has a characteristic absorption peak of 531.5 nm. Results suggested that the coloration mechanism of cobaltoan dolomite is driven by the division and transition of the second outer electrons of the transition metal ion Co^{2+} under the action of the ligand electric field [40]. Electron transitions of cobalt in the dolomite crystal lattice produced selective absorption, leading to the large absorption rate in the green zone centered at about 531.5 nm, which is attributed to the spin-allowed transition of Co^{2+} absorption.

Table 6. The main chemical composition (wt.%) of the pinkish-purple cobaltoan dolomite from the Democratic Republic of Congo, analyzed by EDXRF.

Number	D1-1	D1-2	D1-3	D1-4	D2-1	D3-1	D3-2	D4-1
CaO	55.54	54.93	3.06	3.13	55.40	52.24	53.96	54.05
MgO	39.15	37.58	0.00	0.00	35.67	32.95	33.59	31.93
CoO	1.07	3.97	0.42	0.32	5.48	7.89	7.69	8.70
SiO_2	1.40	1.60	2.92	2.04	1.30	4.32	1.76	1.11
SO_3	0.95	0.78	35.44	33.74	1.10	1.17	0.82	1.16
Al_2O_3	0.00	1.59	3.83	2.04	0.00	1.22	1.76	1.96
CuO	0.72	0.03	52.25	57.78	0.31	0.22	0.02	0.08
Fe_2O_3	0.64	0.28	0.97	0.43	0.02	0.39	0.21	0.55
MnO	0.27	0.13	0.00	0.00	0.61	0.05	0.09	0.27
K_2O	0.04	0.06	0.20	0.08	0.09	0.07	0.02	0.06
total	99.78	100.95	99.09	99.56	99.98	100.52	99.92	99.87

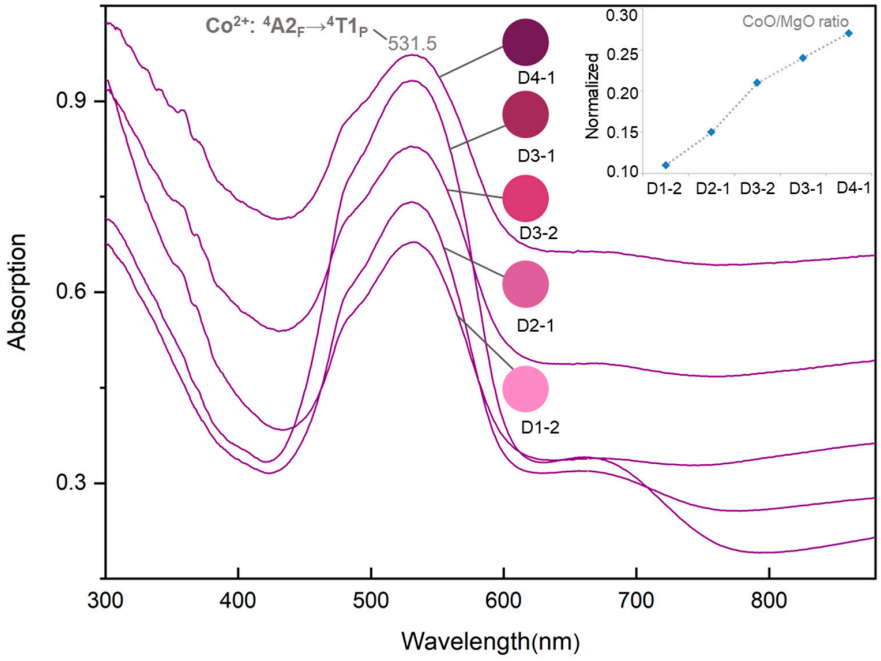

Figure 9. UV-Vis spectra of pinkish-purple cobaltoan dolomite samples. Inset: Normalized trend distribution of the CoO/MgO ratio.

4. Conclusions

In this research, we conducted a systematic study on the gemology, mineralogy, and coloration mechanism of cobaltoan dolomite from the Democratic Republic of Congo,

intending to explore the mineral composition, ascertain the gemological characteristics, and hence be able to provide correct guidance to consumers.

The cobaltoan dolomites samples are generally opaque, mostly with glass luster, and rough in texture. The FTIR microprobe spectra can be assessed to differentiate the common pink to purple gemstones. The pinkish-purple color is mainly caused by the electronic transition of Co^{2+}. UV-Vis spectra showed broad absorption bands at 531.5 nm in the pinkish-purple cobaltoan dolomite. The purple color deepens with the increase in CoO/MgO ratio and the corresponding absorbance of UV-Vis spectra at 531.5 nm, implying that the concentration of Co ions influences the coloration of cobaltoan dolomite.

Cobaltoan dolomite is a mineral aggregate, composed predominantly of Co-rich dolomite with minor amounts of quartz, azurite, and malachite. The degree of fineness and luster differs due to mineral (quartz) impurities in the mineral texture. New data on kolwezite chemical composition were documented, and much clearer backscatter images for the magnesite-spherocobaltite solid solution were presented. Paragenetic minerals occurred in the cobaltoan dolomite, indicating the geological formation in the supergenetic environment.

Author Contributions: Conceptualization, X.-Y.Y.; methodology, Y.Y. and X.-Y.Y.; software, Y.Y.; validation, Y.Y. and X.-Y.Y.; formal analysis, Y.Y.; investigation, Y.Y.; resources, X.-Y.Y.; data curation, Y.Y.; writing—original draft preparation, Y.Y.; writing—review and editing, X.-Y.Y.; visualization, Y.Y.; supervision, X.-Y.Y.; project administration, Y.Y.; funding acquisition, X.-Y.Y. All authors have read and agreed to the published version of the manuscript.

Funding: This study was financially supported by the project from China Geological Survey, grant number DD20190379-88.

Data Availability Statement: Data are contained within the article.

Acknowledgments: The experiments in this article were conducted in the laboratory of the Gemological Institute, China University of Geoscience, Beijing. We would like to thank Long Chu for providing samples and Long Zhengyu and Kamoto Michael and Liu Ziyuan for their kind help in completing this study.

Conflicts of Interest: The authors declare no conflict of interest.

References

1. Siritheerakul, P.; Sangsawong, S. Pink and Reddish Purple COBALTOCALCITE. *Gems Gemol.* **2015**, *51*, 58–59.
2. Zeng, L.; Wan, M.X.; Peng, Y. Order degree of dolomite and its application in petroleum geology. *Nat. Ctas Explor. Dev.* **2004**, *4*, 64–66. (In Chinese)
3. Milton, C.; Axelrod, J.M.; Grimaldi, F.S. New minerals reedmergnerite ($Na_2O{\cdot}B_2O_3{\cdot}6SiO_2$) and eitelite ($Na_2O{\cdot}MgO{\cdot}CO_2$) associated with leucosphenite, shortite, searlesite, and crocidolite in the Green River Formation, Utah. *Geol. Soc. Am. Bull.* **1954**, *65*, 1286–1287.
4. Li, S.R. *Crystallography and Mineralogy*; Geological Publishing House: Beijing, China, 2008. (In Chinese)
5. Hurlbut, C.S. Zincian and plumbian dolomite from Tsumeb, south-west Africa. *Am. Mineral.* **1957**, *42*, 798–803.
6. Fritsch, E.; Rossman, G.R. An update on color in gems. Part 1: Introduction and colors caused by dispersed metal ions. *Gems Gemol.* **1987**, *23*, 126–139. [CrossRef]
7. Du, J.M.; Zhao, X.Z. Geological characteristics and distribution of copper-cobalt deposits in Congo. *Geol. Prospect.* **2010**, *46*, 165–174. (In Chinese)
8. Deliens, M.; Piret, P. La kolwesite, un hydrocarbonate de cuivre et de cobalt analogue a la glaukosphaerite et a la rosasite. *Bull. Mineral.* **1980**, *103*, 179–184. [CrossRef]
9. Gauthier, G.; Deliens, M. Cobalt minerals of the Katanga Crescent, Congo. *Mineral. Rec.* **1999**, *30*, 255–273.
10. Boni, M.; Mondillo, N.; Balassone, G.; Joachimski, M. Zincian dolomite related to supergene alteration in the Iglesias mining district (SW Sardinia). *Int. J. Earth Sci.* **2013**, *102*, 61–71. [CrossRef]
11. Miao, Y.X.; Hao, Y.J.; Dong, S.B. Geological characteristics and genesis of the Kamoya Copper-cobalt deposit in Congo (DRC). *Miner. Explor.* **2014**, *2*, 350–355. (In Chinese)
12. El Desouky, H.A.; Muchez, P.; Dewaele, S. Postorogenic Origin of the Stratiform Cu Mineralization at Lufukwe, Lufilian Foreland, Democratic Republic of Congo. *Econ. Geol.* **2008**, *103*, 555–582. [CrossRef]
13. Li, X.Q.; Mao, J.W.; Yan, Y.L. Regional geology and characteristics of ore deposits in Katangan copper-cobalt belt within Congo (Kinshasa), Central Africa. *Miner. Depos.* **2009**, *28*, 373–376. (In Chinese)

14. Van Langendonck, S.; Muchez, P.; Dewaele, S.; Kaputo Kalubi, A.; Cailteux, J. Petrographic and mineralogical study of the sediment hosted Cu-Co ore deposit at Kambove West in the central part of the Katanga Copperbelt (DRC). *Geol. Belg.* **2013**, *16*, 91–104.
15. Perchiazzi, N.; Dragone, R.; Demitri, N.; Vignola, P. Incorporation of Co in the rosasitemalachite carbonate group of minerals: Crystal structure studies of kolwezite and of synthetic cobaltoan malachites. *Eur. J. Mineral.* **2017**, *30*, 609–620. [CrossRef]
16. Chen, N.X.; Chen, C.; Li, G.G.; Cao, S.Q.; Lu, Y.; Zhang, H. Study on gemological characteristics of pink-purplish red dolomite. *Superhard Mater. Eng.* **2021**, *33*, 47–52. (In Chinese)
17. Douglass, D.L. Cobaltoan Calcite $\frac{1}{4}$ Cobaltoan Dolomite. *Mineral. Rec.* **1992**, *23*, 445.
18. Perchiazzi, N. Crystal structure study of a cobaltoan dolomite from Kolwezi, Democratic Republic of Congo (Article). *Acta Crystallogr. Sect. E Struct. Rep. Online* **2015**, *E71*, i3. [CrossRef]
19. Mincevastefanova, J. First finding of high miscibility in the system $CaMg(CO_3)_2$–$CaCo(CO_3)_2$ in nature. *Geochem. Mineral. Petrol.* **1997**, *32*, 5–16.
20. Barton, I.F.; Yang, H.; Barton, M.D. The mineralogy, geochemistry, and metallurgy of cobalt in the rhombohedral carbonates. *Can. Mineral.* **2014**, *52*, 653–670. [CrossRef]
21. Perchiazzi, N.; Barton, I.F.; Vignola, P. Incorporation of Co in the Dolomite Structure: Coupled Epma and Single Crystal Structural Studies of Co-rich Dolomite from the Tenke-fungurume District, Democratic Republic of Congo. *Can. Mineral.* **2018**, *56*, 151–158. [CrossRef]
22. Ye, X.; Bai, F.; Li, M.; Sun, H. Gemology, Mineralogy, and Spectroscopy of an Attractive Tremolitized Diopside Anorthosite Gem Material from the Philippines: A New Type of Material with Similarities to Dushan Jade. *Minerals* **2021**, *11*, 152. [CrossRef]
23. Bai, F.; Luo, F.; Yang, L.; Zheng, S. Study on gem mineralogy of suji, a new kind of precious jade material. *J. China Non-Met. Miner. Ind.* **2007**, *3*, 71–73. (In Chinese)
24. Chang, L.H.; Chen, M.Y.; Jin, W. *Handbook for Identification of Transparent Mineral Flakes*; Geological Publishing House: Beijing, China, 2006. (In Chinese)
25. Frost, R.L.; Martens, W.N.; Rintoul, L.; Mahmutagic, E.; Kloprogge, J.T. Raman spectroscopic study of azurite and malachite at 298 and 77 K. *J. Raman Spectrosc.* **2002**, *33*, 252–259. [CrossRef]
26. Zhang, R.; Fang, X.; Ju, J.W. Application of Spectrometry on Analysis of Blue and Green Pigments in the Thangka. *J. Light Scatt.* **2020**, *32*, 280–287. (In Chinese)
27. Lu, Z.; He, X.; Lin, C.; Jin, X.; Pan, Y. Identification of Beihong Agate and Nanhong Agate from China Based on Chromaticity and Raman Spectra. *Spectrosc. Spectr. Anal.* **2019**, *39*, 2153–2159.
28. Kingma, K.J.; Hemley, R.J. High-pressure crystalline transformations and amorphization in alpha-quartz. In *AIP Conference Proceedings*; American Institute of Physics: College Park, MD, USA, 1994; Volume 309, pp. 39–42.
29. Shi, X.L. Study on Surface Topography Formation Mechanism and Process in Lapping and Polishing of Tungsten Alloy. Master's Thesis, Dalian University of Technology, Dalian, China, 2020. (In Chinese).
30. Gunasekaran, S.; Anbalagan, G.; Pandi, S. Raman and infrared spectra of carbonates of calcite structure. *J. Raman Spectrosc.* **2006**, *37*, 892–899. [CrossRef]
31. Xu, H.Y.; Yu, X.Y. Pressed Gibbsite and Calcite as A Rhodochrosite Imitation. *Gems Gemol.* **2019**, *55*, 406–415. [CrossRef]
32. Moenke, H.H.W. Vibrational spectra and the crystal-chemical classification of minerals. In *The Infrared Spectra of Minerals*; Farmer, V.C., Ed.; Mineralogical Society of Great Britain and Ireland: London, UK, 1974; pp. 111–118.
33. Gaffey, S.J. Spectral reflectance of carbonate minerals in the visible and near-infrared (0.35~2.55 microns); Calcite, aragonite, and dolomite. *Am. Mineral.* **1986**, *71*, 151–162.
34. Huang, C.K.; Kerr, P.F. Infrared study of the carbonate minerals. *Am. Mineral.* **1960**, *45*, 311–324.
35. Peng, W.S.; Liu, G.K. *Mineral Infrared Spectrum Atlas*; Science Press: Beijing, China, 1982. (In Chinese)
36. Goldsmith, J.R.; Northrop, D.A. Sub solidus phase relations in the systems $CaCO_3$–$MgCO_3$–$CoCO_3$ and $CaCO_3$–$MgCO_3$–$NiCO_3$. *J. Geol.* **1965**, *73*, 817–829. [CrossRef]
37. Zhang, Y. Ore-bearing strata and mineralization characteristics of the Copper-cobalt deposit in Kambvo region, Upper Katanga Province, Congo Technology. *Innov. Appl.* **2017**, *26*, 191–193. (In Chinese)
38. You, X.L.; Jia, W.Q.; Xu, F.; Liu, Y. Mineralogical Characteristics of Ankerite and Mechanisms of Primary and Secondary Origins. *Geoscience* **2018**, *43*, 4046–4055. (In Chinese)
39. Wan, S.Q. New color reactions of cobalt divalent. *Chem. World* **1957**, *9*, 404. (In Chinese)
40. Luo, H.Y.; Wang, C.S.; Liao, S.Y. Theoretical explanation of transition metal ions in gemstones. *Acta Petrol. Mineral.* **2004**, *2*, 177–185. (In Chinese)